



A novel methoxydotrophic metabolism discovered in the hyperthermophilic archaeon *Archaeoglobus fulgidus*

Cornelia U. Welte^{1,2,3} , Rob de Graaf,¹
Paula Dalcin Martins,¹ Robert S. Jansen,¹
Mike S. M. Jetten^{1,2,3} and Julia M. Kurth^{1,3*} 

¹Department of Microbiology, Institute for Water and Wetland Research, Radboud University, Heyendaalseweg 135, Nijmegen, 6525 AJ, The Netherlands.

²Netherlands Earth System Science Center, Utrecht University, Heidelberglaan 2, Utrecht, 3584 CS, The Netherlands.

³Soehngen Institute of Anaerobic Microbiology, Radboud University, Heyendaalseweg 135, Nijmegen, 6525 AJ, The Netherlands.

Summary

Methoxylated aromatic compounds (MACs) are important components of lignin found in significant amounts in the subsurface. Recently, the methanogenic archaeon *Methermicoccus shengliensis* was shown to be able to use a variety of MACs during methoxydotrophic growth. After a molecular survey, we found that the hyperthermophilic non-methanogenic archaeon *Archaeoglobus fulgidus* also encodes genes for a bacterial-like demethoxylation system. In this study, we performed growth and metabolite analysis, and used transcriptomics to investigate the response of *A. fulgidus* during growth on MACs in comparison to growth on lactate. We observed that *A. fulgidus* converts MACs to their hydroxylated derivatives with CO₂ as the main product and sulfate as electron acceptor. Furthermore, we could show that MACs improve the growth of *A. fulgidus* in the presence of organic substrates such as lactate. We also found evidence that other archaea such as *Bathyarchaeota*, *Lokiarchaeota*, *Verstraetearchaeota*, *Korarchaeota*, *Helarchaeota* and *Nezhaarchaeota* encode a demethoxylation system. In summary, we here describe the first non-methanogenic archaeon with the ability to grow on MACs indicating

that methoxydotrophic archaea might play a so far underestimated role in the global carbon cycle.

Introduction

Aromatic compounds are produced by plants, animals and microorganisms and are therefore quite abundant on earth. The polyaromatic compound lignin can be found in significant amounts in the subsurface. Lignin is a major component of photosynthetic biomass and makes up approximately 25% of the dry weight of vascular plants (Zeikus, 1981). It is further estimated that approximately one third of the organic matter present in marine sediments is of terrestrial origin (Burdige, 2005). Overall, lignin analysis indicated that peat and coastal marine sediments contained about 20%–50% of recognizable vascular plant carbon and soils of offshore marine sediments about 0%–10% (Ertel and Hedges, 1984).

There are many possibilities for substitutions on the aromatic ring and one of those possible ring modifications is the addition of methoxy groups resulting in so-called methoxylated aromatic compounds. Lignin contains about 3% methoxy groups respectively (Lee *et al.*, 2019) and methoxylated aromatic compounds as major components of lignin are quite abundant in natural environments (Hedges *et al.*, 1982; Colberg, 1988). Alkyl-methoxyphenols have been found to be typical pyrolysis products of lignin-derived materials (Salmon *et al.*, 1997). It is well known that methoxylated aromatic compounds can be degraded by bacteria. Already in 1979, it was shown that methoxylated aromatic compounds can be converted to methane by the syntrophic association of several anaerobic microorganisms (Healy and Young, 1979). Acetogenic bacteria were the first anaerobes discovered to use methoxylated aromatic compounds for energy conservation (Bache and Pfennig, 1981) via conversion of the methyl group to acetate in the acetyl-CoA (Wood-Ljungdahl) pathway. Some bacteria such as *Sporobacter termitidis* (Grech-Mora *et al.*, 1996), *Sporobacter olearium* (Mechichi *et al.*, 1999) and *Parasporobacterium paucivorans* (Lomans *et al.*, 2001) are able to cleave the aromatic ring after O-demethylation and convert methoxylated aromatic compounds to acetate, methanethiol or dimethylsulfide. O-demethylation is an essential step preceding aromatic ring cleavage. Next to

Received 24 February, 2021; revised 26 April, 2021; accepted 26 April, 2021. *For correspondence. E-mail j.kurth@science.ru.nl; Tel: (+31) 24 3652557.

these ring-cleaving methoxytrophic acetogens, several acetogens have been described to *O*-demethylate methoxylated aromatic compounds and to release the corresponding hydroxylated derivatives into the environment without cleaving the aromatic ring. The methoxy group is transferred into the acetyl-CoA pathway resulting in formation of products such as acetate. Examples of this type of methoxytrophic acetogens are *Sporomusa termitida* (Breznak et al., 1988), *Clostridium thermoaceticum* (Wu et al., 1988) and *Acetobacterium woodii* (Bache and Pfennig, 1981). Acetogens use two methyltransferases, one corrinoid protein and one activating enzyme that recycles the corrinoid protein for transfer of the methyl group from methoxylated compounds (Kaufmann et al., 1997). These enzymes catalyse the *O*-demethylation of the methoxylated compound and methyl transfer to the corrinoid protein as well as subsequent methyl transfer to tetrahydrofolate.

In contrast to the well-studied methoxytrophic growth of acetogenic bacteria, archaea were not well investigated for their ability of converting methoxylated aromatic compounds. It was only recently, that the thermophilic methanogen *Methemicoccus shengliensis* was shown to be able to use a variety of methoxylated aromatic compounds for growth and produces methane from the methoxy group (Mayumi et al., 2016). *M. shengliensis* appears to use a similar *O*-demethylation system as acetogenic bacteria, composed of the so-called Mto proteins (Kurth et al., submitted): MtoB is the *O*-demethylase that transfers the methyl group to the corrinoid protein MtoC, MtoD is the reductive activase of MtoC, and MtoA is a methyltransferase that most likely transfers the methyl group to tetrahydromethanopterin (H₄MPT). Discovery of a methoxytrophic methanogen together with the prevalence of methoxylated compounds on earth lead us to assume that methoxytrophic archaea might play a so far underestimated role in the global carbon cycle, especially in the subsurface (Welte, 2016). To further support this hypothesis, we aimed to identify additional methoxytrophic archaea. A BlastP (NCBI) analysis of the genes encoding the Mto proteins in *M. shengliensis* (BP07_03250-60) revealed that the hyperthermophilic archaeon *Archaeoglobus fulgidus* possesses a similar gene cluster, encoding the Mto proteins (AF_0006-AF_0013). Similar to *Methemicoccus*, *A. fulgidus* (Stetter et al., 1987) belongs to the phylum Euryarchaeota and is related to methanogens. The organism grows anaerobically at extremely high temperatures around 80°C and has been described to be present in marine hydrothermal systems (Stetter et al., 1987) and oil reservoirs (Beeder et al., 1994; Stetter and Huber, 1998). In marine hydrothermal systems, aromatic compounds such as benzenes and phenols have been described as the major organic compounds alongside aliphatic hydrocarbons and carboxylic acids (Konn et al., 2009). Concentrations of about 2–4 µg/g soil have been detected in a hydrothermal

chimney and sediment (Wang et al., 2020). Furthermore, aromatic compounds are a major component (20%–43%) of crude oil (Libes, 2009; Meslé et al., 2013). *A. fulgidus* has been described to couple the reduction of sulfate or thiosulfate with the oxidation of many different organic carbon sources such as small organic acids like lactate, pyruvate, formate (Stetter et al., 1987; Stetter, 1988) or amino acids like phenylalanine (Parthasarathy et al., 2013). The organism also oxidizes fatty acids (C₄ to C₁₈) and *n*-alk-1-enes (C₁₂:1 to C₂₁:1) in the presence of thiosulfate as a terminal electron acceptor producing CO₂ and sulfide (Khelifi et al., 2010). Moreover, *A. fulgidus* has been shown to grow on CO and sulfate thereby producing CO₂, sulfide and acetate (Henstra et al., 2007; Hocking et al., 2015) and on H₂ plus CO₂ with thiosulfate as electron acceptor (Hocking et al., 2014). Furthermore, *A. fulgidus* can use perchlorate and nitrate as electron acceptor during hydrocarbon conversion, indicating its very versatile metabolism (Liebensteiner et al., 2013, 2014). *A. fulgidus* converts organic acids to CO₂ via an acetyl-CoA pathway that involves similar enzymes and cofactors as found in methanogens (Möller-Zinkhan et al., 1989; Möller-Zinkhan and Thauer, 1990). *A. fulgidus* does not encode methyl-CoM reductase and thus lacks the potential to produce methane (Klenk et al., 1997). In this study, we performed growth experiments, analysed the substrate consumption and product formation and the difference in gene expression of *A. fulgidus* grown on methoxy compounds versus lactate. We demonstrate that *A. fulgidus* can grow on methoxylated aromatic compounds and thereby identify the first non-methanogenic archaeon capable of methoxytrophic growth.

Results

Growth of A. fulgidus on methoxylated aromatic compounds versus lactate

After a genome analysis, we identified an *O*-demethylation system in *A. fulgidus*. To experimentally verify if *A. fulgidus* can use this system, we grew the microorganism on 2-methoxyphenol (MP), and compared this to growth on lactate (Fig. 1). Thus, we could show that *A. fulgidus* is able to grow on MP and converts it to 2-hydroxyphenol (HP) (Fig. 1A–C). When 7.5 and 12 mM MP were added, MP was completely converted to HP. However, the increase in doubling time (from 9.4 to 20 h) with higher MP concentrations (Fig. 1A–C) points to an inhibiting or toxic effect of high concentrations of methoxylated aromatics (or their products) on the growth of *A. fulgidus*. At 30 mM MP, no growth could be observed. Overall, growth on MP is comparable to growth on lactate (Fig. 1A, B, D), with a similar doubling time (9.4 vs. 14.4 h) of cultures with 7.5 mM MP and a similar final optical density (OD) of cultures with 12 mM MP

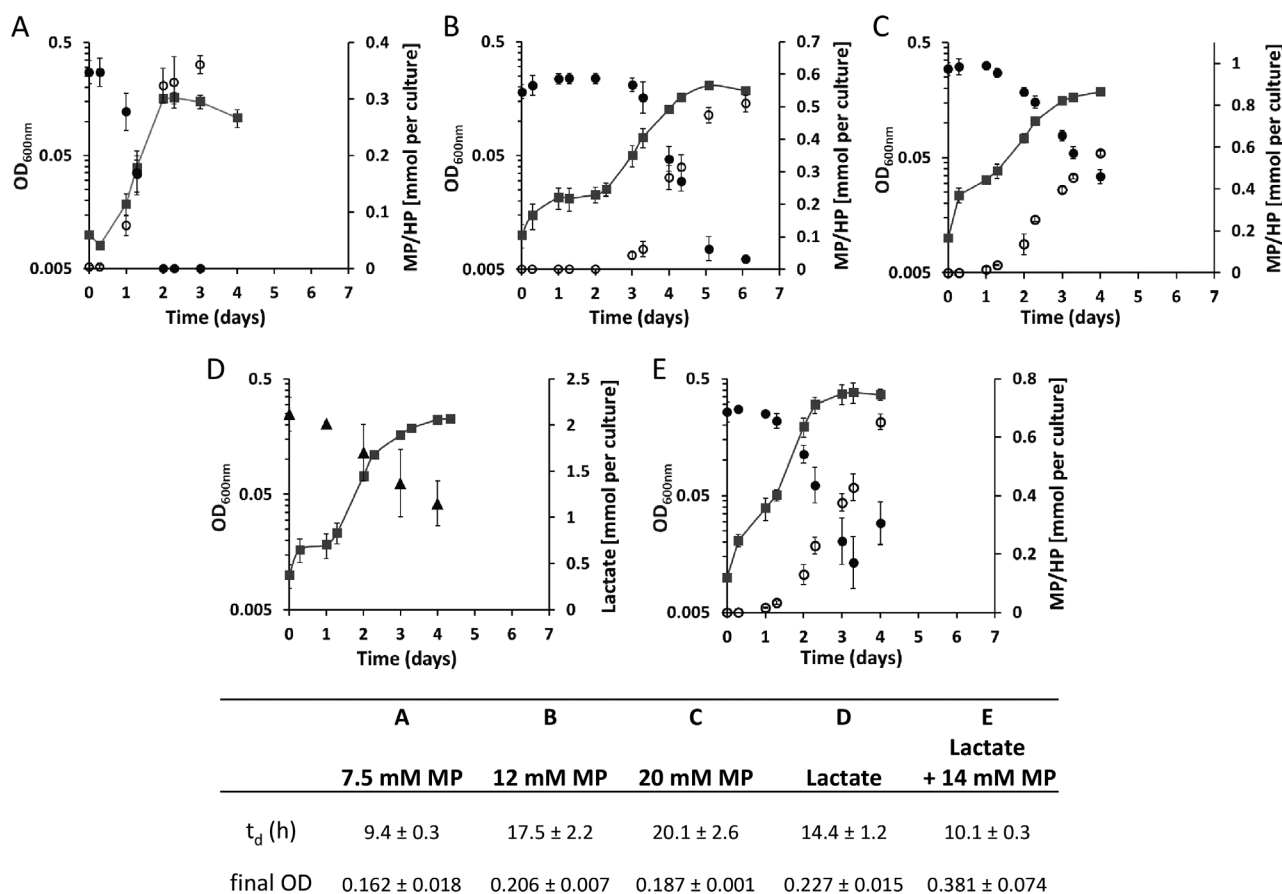


Fig 1. Growth of *A. fulgidus* on 2-methoxyphenol (MP). *A. fulgidus* was grown on either 7.5 mM MP (A), 12 mM MP (B), 20 mM MP (C), 35 mM lactate (D) or 35 mM lactate plus 14 mM MP (E). 2-methoxyphenol and 2-hydroxyphenol were determined by HPLC-UV. Lactate was measured with a colorimetric assay. Grey squares: OD_{600nm} , black circles: 2-methoxyphenol, white circles: 2-hydroxyphenol, black triangles: lactate. Data are presented as mean \pm standard deviation ($n = 3$).

compared to the lactate containing cultures (see below and Fig. 3 for details). When *A. fulgidus* is cultured in medium containing both lactate and MP, MP improves the growth of the organism resulting in a higher final OD and decreased doubling time (Fig. 1E). Next to 2-methoxyphenol, growth on methoxylated aromatics such as 2,6-dimethoxyphenol, methoxyhydroquinone and 2-methoxybenzoate was observed. No growth could be observed on methanol, indicating that there might be no methanol-converting enzyme present in *A. fulgidus*.

The metabolite production and electron acceptor use of *A. fulgidus* during methoxydrotrophic growth were investigated. Therefore CO_2 , acetate, formate, sulfate and sulfide concentrations were measured in experiments with methoxy compounds and lactate (Fig. 2). It appeared that similar amounts of CO_2 are produced in cultures grown on MP and lactate (Fig. 2A). In a resting cell experiment (Fig. 2B), cells grown on lactate produce (a little) more CO_2 in the exponential phase than cells grown on methoxyphenol. The reason might be that –

during growth – also acetate and formate are produced (Fig. 2C and D), but during the resting cell experiment CO_2 might be the main product. Another reason could be that cells grown on methoxyphenol were not that metabolically active during the resting cell experiment due to the toxic effect of MP which might be enhanced in the stabilizing buffer used for the experiment compared to medium. The stabilizing buffer contains potassium phosphate, magnesium sulfate, sodium chloride and sucrose, but lacks ammonium, trace elements, yeast extract and CO_2 . The cells are able to metabolize the substrates in this buffer, but are unable to grow. Extrapolation of the resting cell experiment results would lead to CO_2 production of about $370 \mu mol$ CO_2 per culture produced during growth on MP and $420 \mu mol$ during growth on lactate. In medium without added CO_2 or bicarbonate *A. fulgidus* was only able to grow when lactate was the substrate but not with MP. This indicates that CO_2 is required for assimilation when MP is the substrate. Next to CO_2 , acetate and formate were major products during growth on

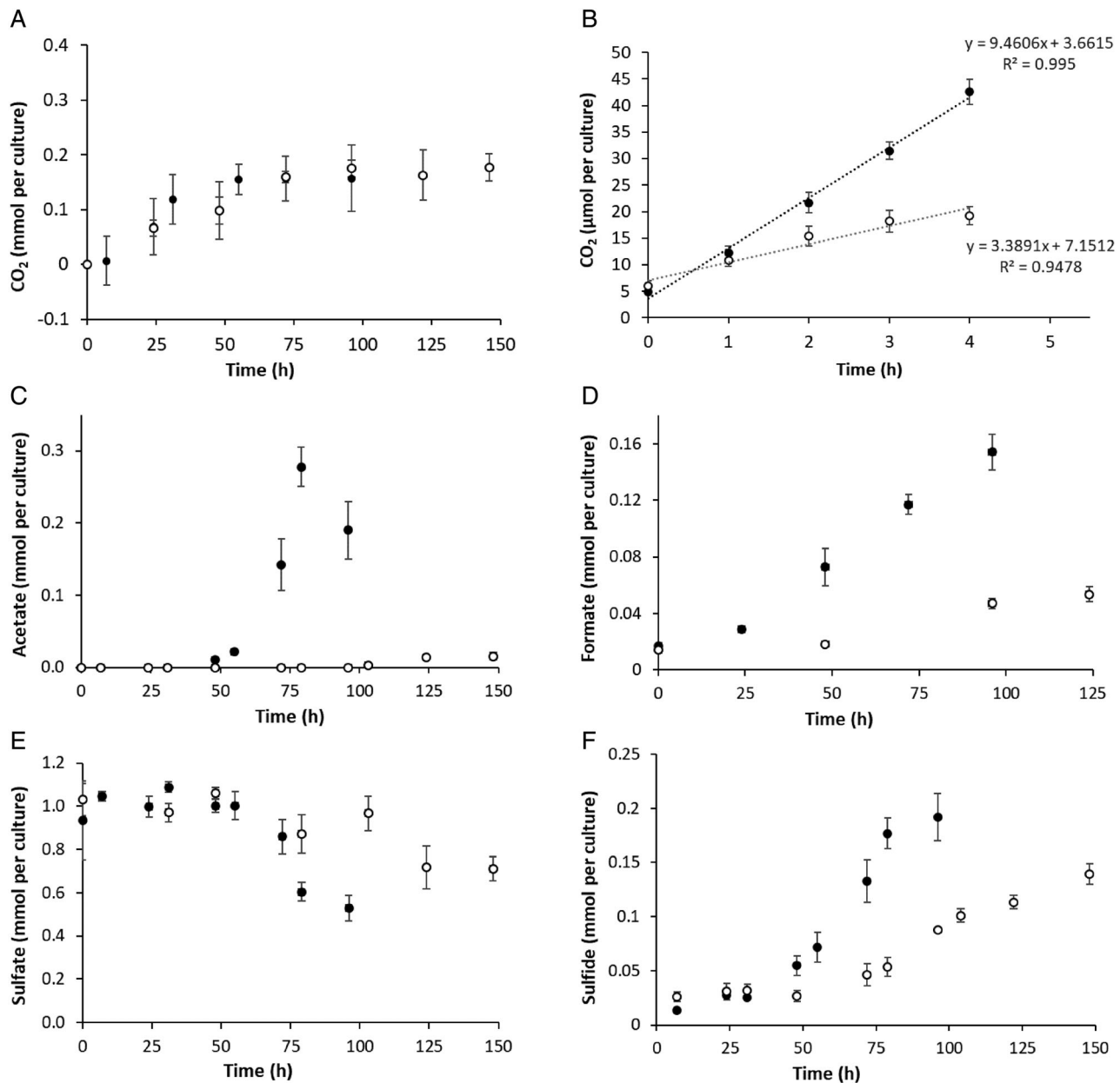


Fig 2. Substrate consumption and product formation during growth of *A. fulgidus* on 12 mM 2-methoxyphenol (grey circles) versus 34 mM lactate (black circles) with 16 mM sulfate as electron acceptor. Samples for (A), (C), (D), (E) and (F) were taken during the growth experiments shown in Fig. 1B and D. Samples for (B) were taken during a resting cell experiment. CO₂ and acetate were measured by gas chromatography and formate, sulfate and sulfide with colorimetric assays. Data are presented as mean \pm standard deviation ($n = 3$).

lactate (Fig. 2C and D). However, during growth on MP only small amounts of acetate ($<20 \mu\text{M}$) and formate ($<50 \mu\text{M}$) were produced (Fig. 2C and D). During both MP and lactate conversion, sulfate is consumed and thereby used as electron acceptor (Fig. 2E). Concomitant sulfide production was also observed (Fig. 2F). Both sulfate consumption and sulfide production were lower in MP grown cells compared to lactate grown cells. In

both cases, lower concentrations of sulfide could be measured than sulfate consumed, which might be due to the reactivity of sulfide and/or the use of sulfide for assimilation.

To get a better insight into the metabolism of *A. fulgidus* grown on MP compared to lactate, the concentrations measured for MP, HP, lactate (all shown in Fig. 1) and for CO₂, acetate, formate, sulfate, sulfide (all shown in Fig. 2) per

culture were incorporated into a schematic overview (Fig. 3). During growth on lactate mainly acetate, CO₂ and formate are produced. Electrons liberated during lactate conversion to pyruvate and acetyl-CoA as well as during the reductive acetyl-CoA pathway, resulting in CO₂ formation, are used for sulfate reduction. During growth on MP, part of the methoxy group is oxidized to CO₂ resulting in liberation of electrons which can be used for sulfate reduction and the other part is combined with CO₂ to acetyl-CoA, from which cell components for assimilation are synthesized. As shown before, only very small amounts of formate or acetate are produced during growth on MP, demonstrating that CO₂ is the main product. Furthermore, it is possible that amino acids such as glutamate that are present in the yeast extract of the medium might be co-assimilated, resulting in mixotrophic growth, as it has been described previously that *A. fulgidus* has the genetic potential to degrade a variety of hydrocarbons and organic acids (Klenk *et al.*, 1997).

A metabolite analysis of *A. fulgidus* cells grown under different conditions (Supporting Information Fig. S1) revealed that *A. fulgidus* cells contained less pyruvate, succinate, citrate, fumarate when grown on MP compared to growth on lactate, which can be partly explained by the growth of *A. fulgidus* on MP and its conversion via the reductive acetyl-CoA pathway instead of growth on organic acids. Furthermore, 2-oxoglutarate was only detected in lactate-grown cultures. In contrast, glutamate was detected in all cultures in comparable amounts.

Transcriptomic analysis

After analysing which products were formed during growth on MP and lactate, we also wanted to investigate how the gene expression differs under the two growth

conditions and which genes are important for methoxydotrophic growth (Supporting Information Tables S1 and S2). The three most upregulated gene clusters under methoxydotrophic growth compared to growth on lactate are shown in Fig. 4. The first gene cluster (Fig. 4A) contains the genes that were identified for *M. shengliensis* to be important for growth on methoxy compounds (Kurth *et al.*, submitted). This gene cluster encodes the O-demethylase MtoB, which is responsible for O-demethylation of the methoxy compound, the cobalamin binding protein MtoC that accepts the methyl group from MtoB, the reductive activase of MtoC named MtoD, the methyl transferase MtoA which most likely transfers the methyl group from MtoC to tetrahydromethanopterin (H₄MPT) and major facilitator superfamily transporters that might be involved in import of the methoxylated aromatic compounds and export of the hydroxylated derivatives. The role of these enzymes is depicted in Fig. 5.

Another highly upregulated gene cluster encodes for two F₄₂₀-non-reducing hydrogenases, Vht and Vhu, and for a heterodisulfide reductase (Hdr) complex. The cytoplasmic Vhu hydrogenase (also referred to as Mvh hydrogenase) is assumed to be associated with the Hdr complex (Hocking *et al.*, 2014). The Vht hydrogenase contains a membrane subunit and is most likely located in the pseudoperiplasm. As no hydrogen gas was added to the cultures and no production of hydrogen could be detected, there is most likely an internal hydrogen cycling occurring in the cells. H₂ might be produced by the Hdr/Vhu complex and reoxidized by the periplasmic Vht hydrogenase, contributing to the proton gradient and reducing menaquinone. The third gene cluster that is highly overexpressed under MP growth encodes the 2-oxoglutarate/2-oxoacid ferredoxin oxidoreductase

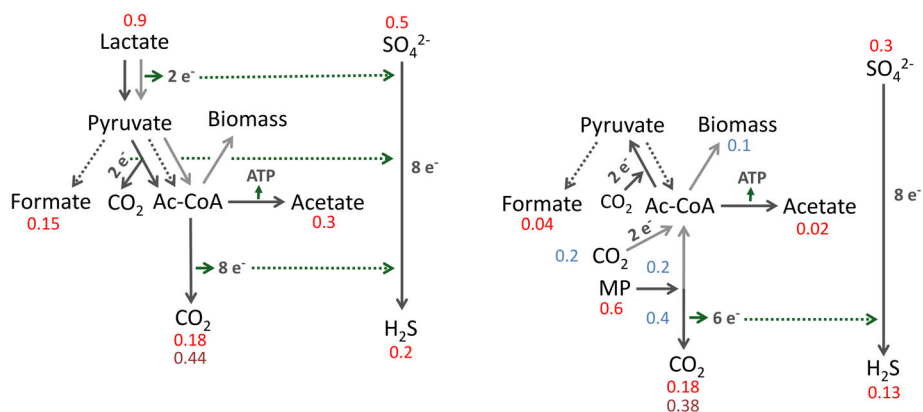


Fig 3. Substrate consumption/product formation during growth of *A. fulgidus* on 12 mM 2-methoxyphenol versus 34 mM lactate. Values refer to mmol per culture. Red values are based on experimental measurements (see Fig. 2; dark red values refer to resting cell experiment) and blue values are based on estimations (Compensation for the experimentally determined values for metabolites such as CO₂ and MP). Dark green dotted arrows visualize electrons liberated during carbon metabolism that are consumed during sulfate reduction. Sulfide is most likely underestimated as sulfide reacts with other medium/cell components and is also used for assimilation.

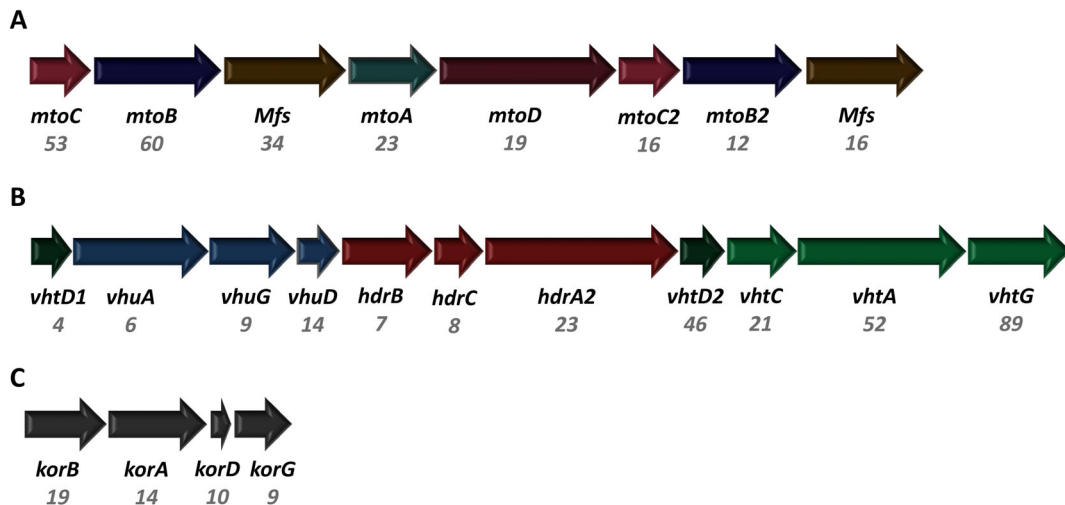


Fig 4. Gene clusters upregulated under growth on MP versus lactate with corresponding fold change values. The gene clusters depicted here encode (A) proteins involved in demethoxylation (AF_0006–13), (B) hydrogenases (AF_1371–81) and (C) the 2-oxoglutarate/2-oxoacid ferredoxin oxidoreductase KorABDG (AF_0468–71). MtoC: Cobalamin binding protein, MtoD: corrinoid activator protein, MtoB: O-demethylase, MtoA: methyl transferase, MFS: major facilitator superfamily transporter, HdrABC: soluble heterodisulfide reductase, Vht and Vhu: F_{420} -nonreducing hydrogenase, KorABDG: 2-oxoglutarate/2-oxoacid ferredoxin oxidoreductase. The difference in gene expression of those genes after growth on MP or lactate is shown in Supporting Information Table S2. Fold change values are depicted in grey. [Color figure can be viewed at wileyonlinelibrary.com]

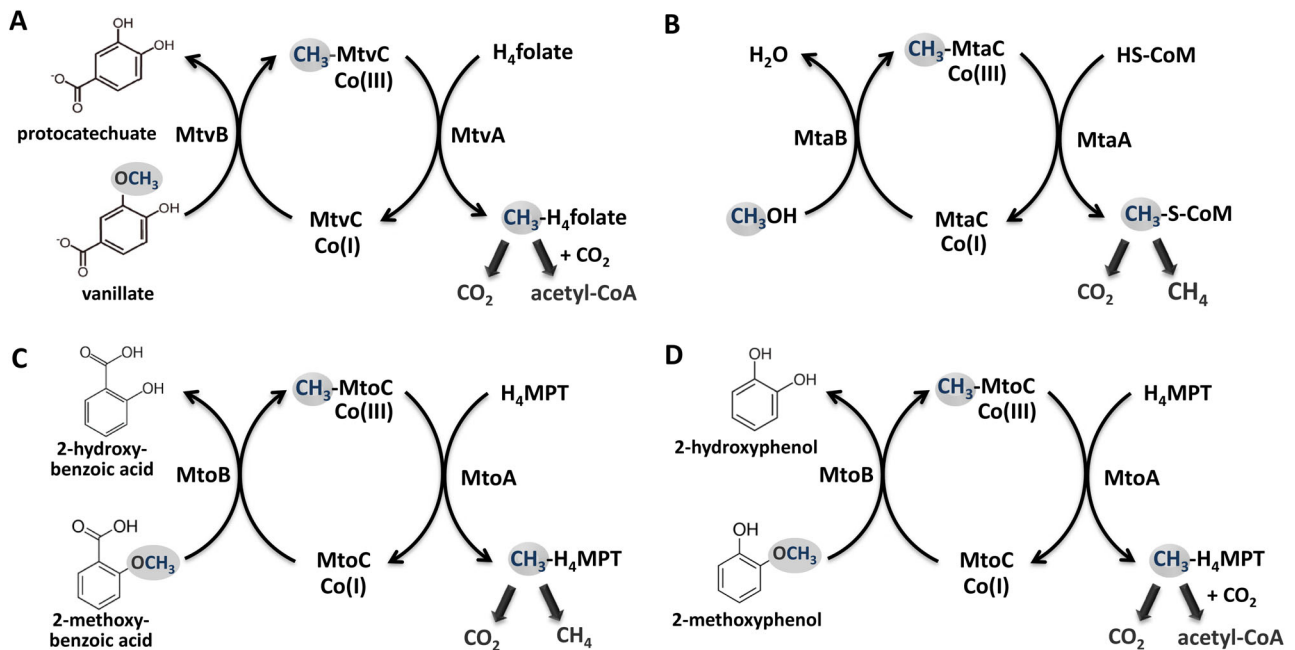


Fig 5. Demethylation and demethoxylation pathways of methoxytrophic archaea in comparison to methylotrophic methanogens and acetogenic bacteria. (A) Demethoxylation pathway as described for the acetogenic bacterium *Moorella thermoacetica*, modified from Pierce *et al.* (Pierce *et al.*, 2008). (B) Demethylation pathway in methanogenic archaea when using methanol as substrate. (C) Demethoxylation pathway of the methanogen *M. shengliensis* (Mayumi *et al.*, 2016; Kurth *et al.*, submitted). (D) Tentative demethoxylation pathway of *A. fulgidus*. Genomic and transcriptomic analysis revealed cobalamin binding protein MtoC (AF_0006) and its activator MtoD (AF_0010), O-demethylase MtoB (AF_0007) and methyl transferase MtoA (AF_0009) to be essential for growth of *A. fulgidus* on methoxylated aromatic compounds. CoM: coenzyme M, H_4 folate: tetrahydrofolate, CO(III): cobalamin binding protein, H_4 MPT: tetrahydromethanopterin. [Color figure can be viewed at wileyonlinelibrary.com]

KorABDG. This enzyme can be part of the tricarboxylic acid (TCA) cycle and catalyses the reversible conversion of 2-oxoglutarate to succinyl-CoA and reduction of

ferredoxin, therefore potentially playing a role in regenerating/providing reducing equivalents. The 2-oxoglutarate might derive from glutamate which is

present in the yeast extract provided to the medium. Next to those three gene clusters also genes encoding for proteins involved in lipid metabolism, more precisely fatty acid activation and β -oxidation, are highly upregulated. Those highly upregulated genes encode for proteins such as the long-chain-fatty-acid-CoA ligase FadD, the acyl-CoA dehydrogenase Acd, the enoyl-CoA hydratase Fad, the 3-hydroxyacyl-CoA dehydrogenase Hbd, the 3-ketoacyl-CoA thiolase AcaB and FadA, the medium-chain acyl-CoA ligase AlkK and the 4-hydroxybutyrate CoA transferase Cat2 (Fig. 6, Supporting Information Tables S1 and S2). Other genes that are strongly induced under MP growth are genes encoding branched-chain amino acid ABC transporter subunits (Supporting Information Table S2) involved in amino-acid uptake, genes encoding acyl-CoA synthetase Acs, which might play a role in acetate activation or fatty acid activation, as well as genes encoding putative acyl-CoA transferase/formyl-CoA transferases. Similar observations were made in a transcriptomic study with *A. fulgidus* cell grown on H_2/CO_2 versus lactate (Hocking *et al.*, 2014) and might therefore be associated with the growth of *A. fulgidus* on substrates other than organic acids and putatively the co-assimilation of lipids, amino acids and other organic compounds, resulting in mixotrophic growth.

Genes that are downregulated during growth on MP (Supporting Information Table S3) encode proteins involved in ammonia uptake (Amt) and glutamine metabolism/nitrogen regulation (GlnA, GlnB), ferrous iron transport (FeoB), phosphate transport (PstSABC) as well as pyruvate metabolism (PorABDG). Ammonia and glutamine metabolism might be downregulated because of co-assimilation of amino acids such as glutamate, which would match with the upregulation of *korABDG*. Genes encoding the pyruvate ferredoxin oxidoreductase PorABDG are most likely downregulated as less pyruvate is produced due to the lack of lactate conversion. The downregulation of genes involved in ferrous iron and phosphate uptake might correlate with a decreased production of iron-sulfur and polyphosphate bodies that have been described for *A. fulgidus* cells (Toso *et al.*, 2016). The iron-sulfur bodies store iron, sulfur plus copper and the polyphosphate bodies contain phosphorus plus magnesium, calcium, and aluminium. Those iron-sulfur and polyphosphate bodies are assumed to be involved in energy storage and/or metal sequestration/detoxification.

Proteins involved in the metabolism of methoxylated aromatics, acetyl-CoA/Wood-Ljungdahl pathway, lactate metabolism, TCA cycle, sulfate reduction, energy metabolism and regeneration of reducing equivalents are shown in Fig. 7 (for details see also Fig. 6 and Supporting Information Table S1) with the respective transcription profile for growth on MP versus lactate.

There is no significant change in transcription regarding genes encoding proteins involved in sulfate reduction and acetyl-CoA pathway. This matches with the observation that sulfate serves as electron acceptor and CO_2 is produced under both growth conditions. Regarding energy metabolism and regeneration of reducing equivalents, only genes encoding for the Hdr complex and the two hydrogenases (Vht and Vhu) are upregulated on MP. In view of the TCA cycle, some of the genes encoding proteins involved in the stepwise conversion from 2-oxoglutarate to pyruvate are upregulated (*KorABDG*, *SdhABCD*, *Fum*, *Pyc*), whereas genes encoding proteins involved in citrate and isocitrate formation are downregulated (*Cit*, *Acn*). Those observations are discussed below.

Discussion

Methoxydrotrophic growth – O-demethylation of methoxylated aromatic compounds

In this study, we demonstrate that *A. fulgidus* can grow on methoxylated aromatic compounds such as 2-methoxyphenol. Similar to some acetogenic bacteria, e.g. *Sporomusa termitida* (Breznak *et al.*, 1988), *Clostridium thermoaceticum* (Wu *et al.*, 1988) and *Acetobacterium woodii* (Bache and Pfennig, 1981), as well as the methanogenic archaeon *M. shengliensis* (Kurth *et al.*, submitted; Mayumi *et al.*, 2016), *A. fulgidus* converts methoxylated aromatic compounds to their hydroxylated derivatives (Fig. 1). Surprisingly, both the archaea *M. shengliensis* and *A. fulgidus* use an O-demethylation system that is similar to that of acetogenic bacteria (Fig. 5 and Kurth *et al.*, submitted). The enzymes that are part of this system are encoded in a gene cluster that is highly induced under methoxydrotrophic conditions (Fig. 4A). These MtoABCD proteins facilitate O-demethylation of the methoxy compound and methyl transfer via a corrinoid protein to most probably tetrahydromethanopterin (H_4MPT) (Kurth *et al.*, submitted). The acetyl-CoA pathway of *A. fulgidus* has been shown to rather involve tetrahydromethanopterin than tetrahydrofolate as C1-carrier (Möller-Zinkhan *et al.*, 1989) which differs to acetogenic bacteria but strengthens the hypothesis that MtoA transfers the methyl group to H_4MPT in *A. fulgidus*. The produced methyl- H_4MPT can then be oxidized to CO_2 via the reductive acetyl-CoA pathway, generating reducing equivalents which provide electrons for sulfate reduction directly via ferredoxin or indirectly via reduced menaquinone (Fig. 7). We could further show that growth characteristics for MP as substrate were comparable to those for lactate (Fig. 1). However, MP concentrations of 12 mM and higher had an inhibiting effect on growth,

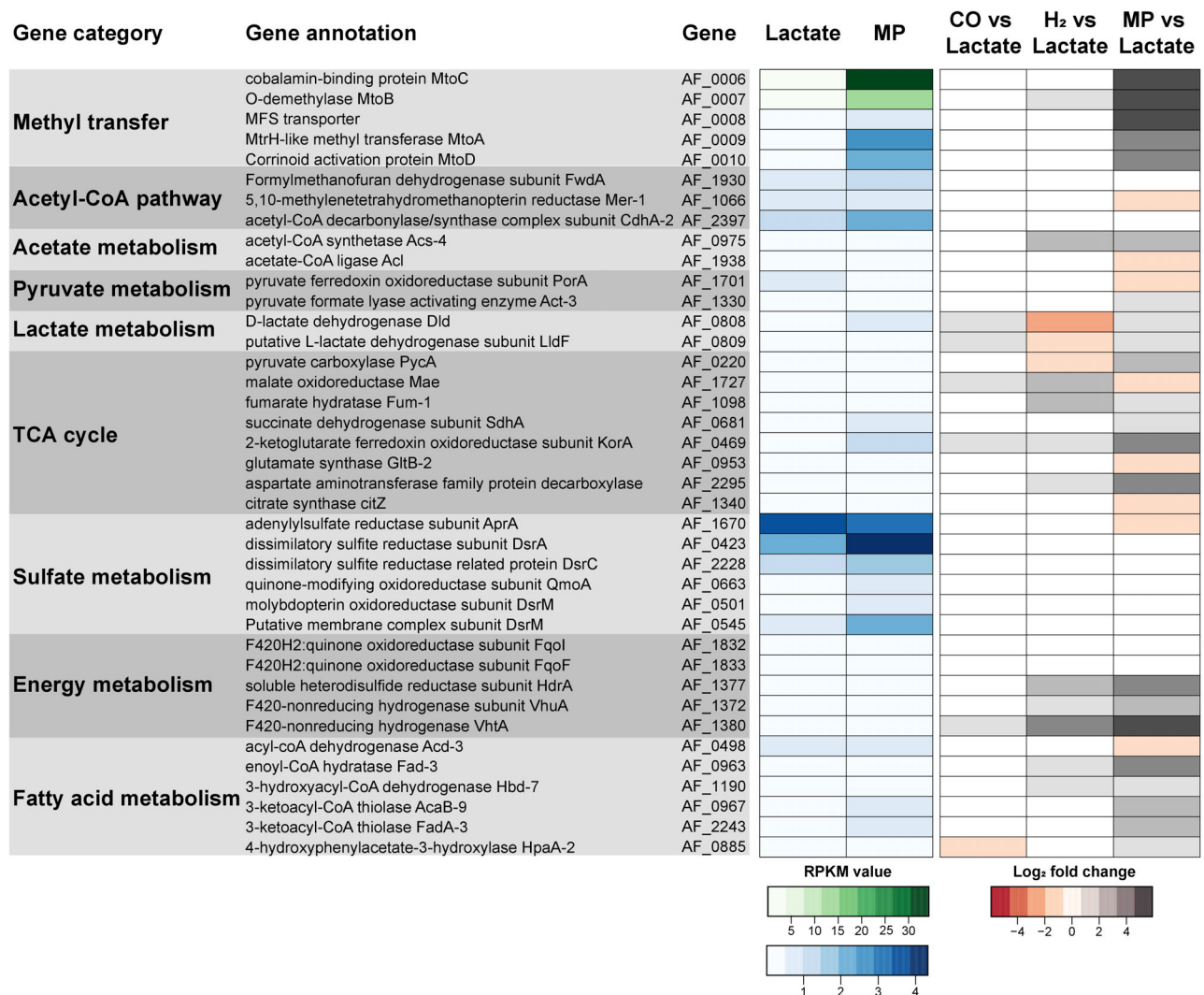


Fig 6. Comparison of gene expression during growth of *A. fulgidus* on lactate to growth on 2-methoxyphenol, H₂/CO₂ or CO. RPKM (reads per kilobase transcript per million mapped reads) values were normalized to the average S3 ribosomal protein (gene AF_1919) RPKM under growth on lactate or 2-methoxyphenol (MP). RPKM values for AF_0006 and AF_0007 are depicted with a different scale (green shades) than the other genes (blue shades). Log₂fold change values are shown for MP versus lactate (this study), H₂/CO₂ versus lactate (Hocking *et al.*, 2014) and CO versus lactate (Hocking *et al.*, 2015) (red/grey shades). Non-normalized RPKM values and log₂fold change values can also be found in Supporting Information Tables S1–S3.

which might be due to the toxic effect of aromatic hydrocarbons or their products. At lower concentrations, however, methoxy compounds improved the growth of *A. fulgidus* in the presence of lactate. As *A. fulgidus* thrives in environments such as hydrothermal marine systems (Stetter *et al.*, 1987) and oil reservoirs (Beeder *et al.*, 1994; Stetter and Huber, 1998) where aromatic compounds are present (Konn *et al.*, 2009; Libes, 2009; Meslé *et al.*, 2013) the ability to use methoxylated aromatics for growth might lead to a growth advantage over organisms that are incapable of methoxytrophic growth. Furthermore, the use of methoxylated aromatics as co-substrate to organic acids such as acetate or lactate, amino acids, fatty acids or sugars might be more

prevalent than so far assumed in marine environments and subsurface sediments as methoxy compounds are quite abundant on earth.

Bioinformatic analysis revealed that also other archaea that thrive in hydrothermal deep-sea sediments such as members of the phyla Bathyarchaeota, Lokiarchaeota, Korarchaeota, Helarchaeota, Verstraetearchaeota and Nezharchaeota contain *mtoABC* homologues in their genomes (Fig. 8). The latter three organisms are assumed to be involved in methane and/or alkane metabolism (Hua *et al.*, 2019; Seitz *et al.*, 2019; Wang *et al.*, 2019). Bathyarchaeota are very abundant in marine subsurface sediments and have the potential for acetogenesis and for the fermentative utilization of a

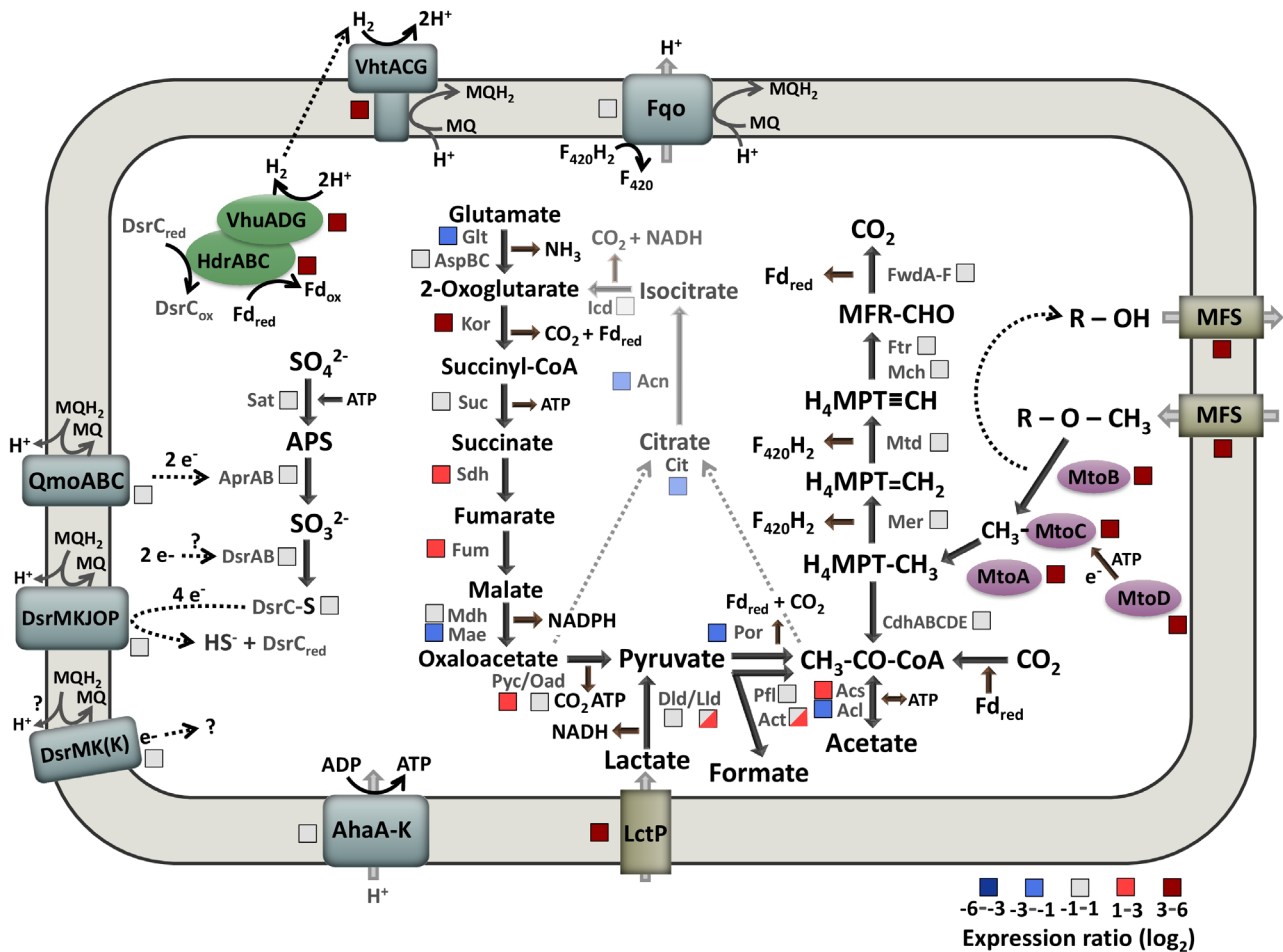


Fig 7. Tentative pathway for methoxytrophic growth in *A. fulgidus*. RPKM and log₂ fold change values for all proteins shown in this figure are included in Supporting Information Table S1. Genes encoding the following enzymes can be found in *A. fulgidus* VC-16: Formylmethanofuran dehydrogenase FwdA-F (AF_0177, AF_1644, AF_1649-51, AF_1928-31), formylmethanofuran-tetrahydromethanopterin formyl-transferase Ftr (AF_2073 & AF_2207), methenyl-tetrahydromethanopterin cyclohydrolase Mch (AF_1935), methylenetetrahydromethanopterin dehydrogenase Mtd (AF_0714), 5,10-methylenetetrahydromethanopterin reductase Mer (AF_1066 & AF_1196), acetyl-CoA decarboxylase/synthase CODH/ACS complex CdhABCDE (AF_0376/7/9, AF_1100/1, AF_2397/8), acetyl-CoA synthetase Acs1-5 (AF_0197, AF_0366, AF_0677, AF_0975, AF_0976) and acetate-CoA ligase Acl (AF_1211 & AF_1938), pyruvate ferredoxin oxidoreductase PorABDG (AF_1699-1702), pyruvate formate lyase PflCD (AF_1449/50), PflX (AF_1961) and Act-1-4 (AF_0117, AF_0918, AF_1330, AF_2278), D-lactate dehydrogenase Dld (AF_0394 & AF_0808), L-lactate dehydrogenase LldD (AF_0807) and LldEFG (AF_0809-AF_0811), lactate permease lctP (AF_0806), pyruvate carboxylase PycA (AF_0220) and oxaloacetate decarboxylase Oad (AF_1252), malate dehydrogenase MdhA (AF_0855) and malate oxidoreductase Mae (AF_1727), fumarate hydratase Fum-1/2 (AF_1098/9), succinate dehydrogenase SdhA-D (AF_0681-4), succinyl-CoA synthetase SucCD (AF_1539/40 & AF_2185/6), 2-oxoglutarate/2-oxoacid ferredoxin oxidoreductase KorABDG (AF_0468-71), glutamate synthase GltB1-3 (AF_0952-4), aspartate aminotransferase AspBC (AF_0409, AF_1623, AF_2129, AF_2366, AF_1417), isocitrate dehydrogenase Icd (AF_0647), aconitase Acn (AF_1963), citrate synthase CitZ (AF_1340), sulfate adenylyltransferase Sat (AF_1667), adenylylsulfate reductase AprAB (AF_1669-70), dissimilatory sulfite reductase DsrAB (AF_0423-4), DsrC (AF_2228), quinone-modifying oxidoreductase QmoABC (AF_0661-3), molybdopterin oxidoreductase DsrMKJOP (AF_0499-503), DsrMK(K) (AF_0543-5), F₄₂₀H₂:quinone oxidoreductase FqoJKMLNABCDHIF (AF_1823-33), soluble heterodisulfide reductase HdrABC (AF_1375-7), F₄₂₀-non-reducing hydrogenase VhuADG (AF_1372-4), F₄₂₀-non-reducing hydrogenase VhtACDG (AF_1378-81), ATP synthase AtpA-K (AF_1158-68), cobalamin binding protein MtoC (AF_0006) and its activator MtoD (AF_0010), O-demethylase MtoB (AF_0007) and methyl transferase MtoA (AF_0009), MFS transporters (AF_0008 & AF_0013). H₄MPT: tetrahydromethanopterin, MQH₂: reduced menaquinone (MQ), MFR: methanofuran, Fd: ferredoxin, F₄₂₀H₂: reduced coenzyme F₄₂₀, MFS: major facilitator superfamily transporter. Expression ratio shown for *A. fulgidus* grown on MP versus lactate.

variety of organic substrates (He *et al.*, 2016). Furthermore, they have been described to be able to grow on lignin (Yu *et al.*, 2018). Also for Lokiarchaeota, it is assumed that they have the potential to degrade lignin

besides other substrates, such as humic acids, lactate, aromatic compounds and proteins (Yin *et al.*, 2020). The presence of *mto* homologues in those archaea therefore might suggest that they are able to grow on MACs.

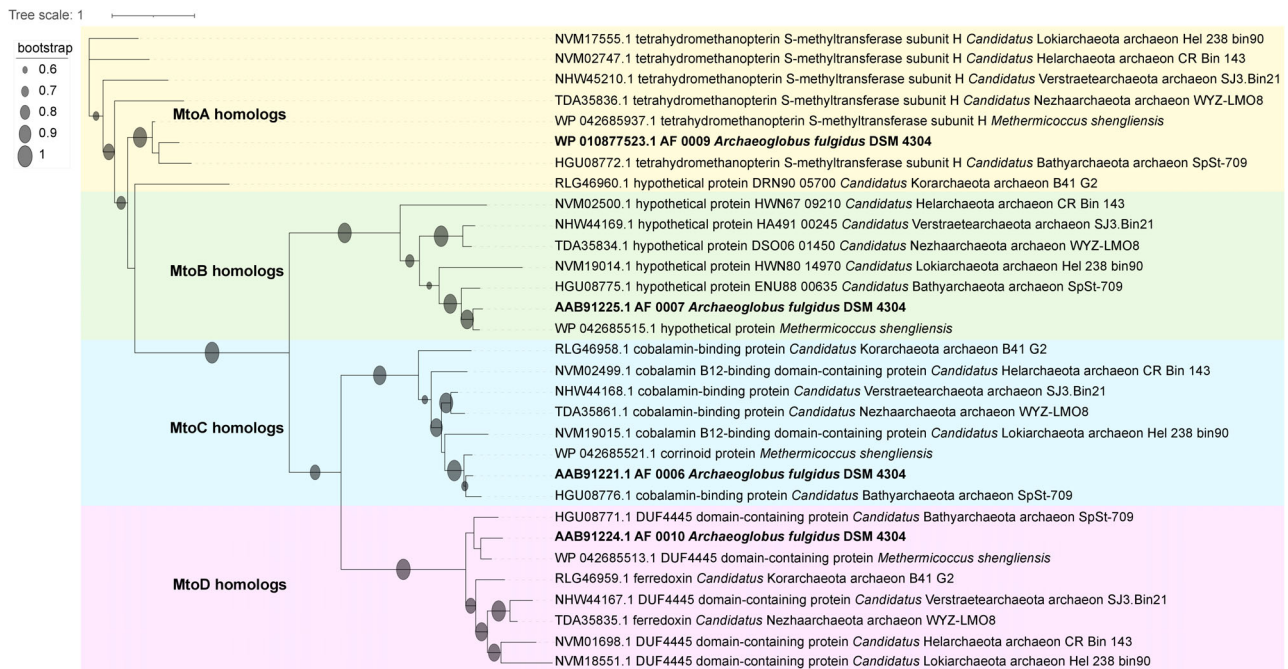


Fig 8. Phylogenetic tree of Mto proteins from *A. fulgidus* and putative homologues from other archaea. The tree was generated with FastTree using the Jones-Taylor-Thorton maximum likelihood model. Sequence accession numbers from NCBI are provided in the tree.

Metabolism – products formed and electron acceptor used during methoxydrotrophic growth

We observed that next to 2-hydroxyphenol, CO₂ is the main carbon compound produced by *A. fulgidus* during growth on MP, whereas substantial amounts of acetate and formate are produced besides CO₂ during growth on lactate (Fig. 2). During methoxydrotrophic growth, the methoxy/methyl group ends up as methyl-H₄MPT in the α -acetyl-CoA pathway and is then either oxidized to CO₂ resulting in generation of reducing equivalents or combined with CO₂ to form acetyl-CoA which is required for assimilation (Fig. 3). When lactate is used as carbon and energy source, reducing equivalents are generated during oxidation of lactate to acetyl-CoA via pyruvate, but also during oxidation of acetyl-CoA to CO₂ in the reductive acetyl-CoA pathway. Moreover, ATP can directly be generated from the conversion of acetyl-CoA to acetate. Formate and CO₂ are side products from the oxidation of pyruvate to acetyl-CoA. The produced acetyl-CoA can further also be used for assimilation. Production of acetate, formate, and CO₂ from lactate has already been shown previously and the stoichiometry of the catabolic reaction seems to strongly depend on the sulfate concentration (Habicht *et al.*, 2005). In our study, sulfate was reduced to sulfide under both growth conditions and therefore serves as electron acceptor.

Energy metabolism and regeneration of reducing equivalents

Regarding energy metabolism and regeneration of reducing equivalents, mainly genes encoding for the Hdr complex and the two hydrogenases (Vht and Vhu) are upregulated (Fig. 7 and Supporting Information Table S1). This might be due to an increased concentration of reduced ferredoxin (Fd_{red}) in the cells which most likely result from increased production of Fd_{red} in the reductive acetyl-CoA pathway (CO₂ is the main carbon compound produced during growth on MP), the putative increased production of Fd_{red} by 2-oxoglutarate ferredoxin oxidoreductase KorABDG (upregulation of *korABDG* genes) and a decrease in sulfate reduction (less sulfate is reduced during growth on MP) which might involve Fd_{red} as electron donor as Qmo and DsrAB have Fd binding sites (Hocking *et al.*, 2014). Although less Fd_{red} is assumed to be produced by pyruvate ferredoxin oxidoreductase PorABDG (downregulation of *porABDG* genes), there might still be an increased concentration of Fd_{red} in cells grown on MP compared to cells grown on lactate. Fd_{red} is the most likely electron donor for the Hdr/Vhu complex, as cultures are not grown on H₂. Reoxidation of Fd_{red} by the Hdr/Vhu complex putatively involves oxidation of DsrC (two SH-groups) and reduction of H⁺ to H₂, which could then be oxidized

by the pseudoperiplasmic Vht hydrogenase contributing to the proton motive force. The internal hydrogen cycling under methoxydrotrophic growth conditions is supported by the observation that there was no net production or consumption of hydrogen in the cultures. For the sulfate-reducing bacterium *Desulfovibrio gigas*, it has been described that hydrogen cycling takes place in lactate-grown cultures and led to the assumption that hydrogen cycling with vectorial electron transfer might be a general mechanism for energy coupling in sulfate-reducing bacteria (Odom and Peck, 1981). However, in *A. fulgidus* the hydrogenases are hardly induced in lactate grown cultures (this study and Hocking *et al.*, 2014; see also Fig. 6) indicating that hydrogen cycling only plays a role when the organism grows on substrates other than organic acids and H₂. Under growth on H₂/CO₂ and partly also under growth on CO compared to growth on lactate the genes encoding the aforementioned hydrogenases and Hdr proteins are also upregulated (Fig. 6 and Hocking *et al.*, 2014, 2015) indicating that they play a general role in energy metabolism and regeneration of reducing equivalents during autotrophic or mixotrophic growth of *A. fulgidus*. Internal hydrogen cycling has also been observed in acetogens such as *Acetobacterium woodii* (Wiechmann *et al.*, 2020).

Regarding the TCA cycle, some of the genes encoding proteins involved in the stepwise conversion from 2-oxoglutarate to pyruvate are upregulated (KorABDG, SdhABCD, Fum, Pyc), whereas genes encoding proteins involved in citrate and isocitrate formation are downregulated (Cit, Acn) (for comparison Fig. 7 and Supporting Information Table S1). This might be due to the upregulation of genes encoding the 2-oxoglutarate ferredoxin oxidoreductase KorABDG, which might play a role in Fd_{red} production and therefore providing/regenerating reducing equivalents. The metabolite analysis of *A. fulgidus* cells (Supporting Information Fig. S1) revealed that *A. fulgidus* cells contained less of some TCA cycle metabolites such as succinate, or fumarate when grown on MP compared to growth on lactate. Next to the lack of lactate and pyruvate also an upregulation of genes encoding for TCA cycle proteins might explain this finding and fits to the transcriptomic results mentioned before. The absence of 2-oxoglutarate in MP-grown cells (Supporting Information Fig. S1) is in agreement with the upregulation of the *korABDG* genes and further indicates that KorABDG indeed converts 2-oxoglutarate to succinyl-CoA resulting in Fd_{red} production and does not primarily catalyse the reverse reaction. Furthermore, less Fd_{red} is produced by PorABDG due to the lack of pyruvate providing compounds such as lactate which was evidenced in this study by downregulation of the *porABDG* genes and the metabolite analysis (Supporting Information Table S1 and Fig. S1). KorABDG might

compensate for that by providing Fd_{red}. However, the source of 2-oxoglutarate could not be detected yet. We assume that glutamate or other amino acids might be converted to 2-oxoglutarate as amino acids are present in the yeast extract provided to the medium. However, putative glutamate converting enzymes such as the aspartate aminotransferase AspBC are not upregulated under methoxydrotrophic growth. However, a quarter of the *A. fulgidus* genome encodes functionally uncharacterized proteins (Klenk *et al.*, 1997) so we might have overlooked a hitherto undescribed glutamate converting enzyme. A gene encoding an aspartate aminotransferase family protein/glutamate decarboxylase is highly upregulated on MP (AF_2295) which could have a role in glutamate conversion. It might also be possible that glutamate is transformed into γ -aminobutyrate and that KorABDG plays a role in the GABA shunt. For *Mycobacterium tuberculosis* it has been shown that α -ketoglutarate dehydrogenase defends the bacterium against glutamate anaplerosis and oxidative stress caused by reactive nitrogen species (Maksymiuk *et al.*, 2015) indicating that the genes encoding enzyme might be induced during methoxydrotrophic growth of *A. fulgidus* due to stress response. Furthermore, this enzyme seems to have a more important role during growth on MACs than growth on H₂/CO₂ or CO as genes encoding this enzyme are not upregulated under those conditions (Hocking *et al.*, 2014, 2015) (see also Fig. 6) demonstrating that its upregulation might correlate with a stress response caused by methoxydrotrophic growth. Also, the genes encoding the cytochrome *bd* ubiquinol oxidase subunits AF_2296 and AF_2297 are strongly upregulated under methoxydrotrophic growth (Supporting Information Table S2) which might be due to an oxidative stress response.

Lipid and amino acid metabolism

A. fulgidus possesses 57 genes encoding β -oxidation enzymes indicating that the organism is able to degrade a variety of hydrocarbons and organic acids (Klenk *et al.*, 1997). In this study, we observed that a vast number of genes encoding for proteins involved in lipid metabolism, amino acid uptake, and acetate/fatty acid activation are upregulated in *A. fulgidus* cells grown on methoxylated aromatics versus lactate. In a transcriptomic study with *A. fulgidus* cells grown on H₂/CO₂ versus lactate, similar observations were made (Hocking *et al.*, 2014; see also Fig. 6). The upregulation of those genes might enable the organism to co-assimilate lipids, amino acids and other organic compounds, resulting in mixotrophic growth. Furthermore, some of the upregulated genes (AF_0333, AF_0885, AF_1027) might encode for enzymes that are part of a

3-hydroxypropionate/4-hydroxybutyrate (3HP/4HB) cycle (Hocking *et al.*, 2014) identified in *Metallosphaera sedula* (Berg *et al.*, 2007) and might represent a secondary carbon fixation pathway in *A. fulgidus*. However, in a study with *Archaeoglobus lithotrophicus*, no enzyme activities associated with the dicarboxylate/hydroxybutyrate or the hydroxypropionate/hydroxybutyrate cycles were detected (Estelmann *et al.*, 2011).

Conclusion

In summary, we describe the first non-methanogenic methoxytrophic archaeon. Similar to the so far first and only described methoxytrophic archaeon *M. shengliensis*, which uses methoxylated aromatics for methane production, a bacterial-like demethoxylation system is used in *A. fulgidus*. In contrast to *M. shengliensis*, *A. fulgidus* converts the methoxy group primarily to CO₂ and not to CH₄ by using the reductive acetyl-CoA pathway, hereby representing a novel type of archaeal metabolism. We showed that *A. fulgidus* can grow on a variety of methoxylated aromatic compounds with a comparable growth rate and growth yield as on lactate and we demonstrated that those compounds improve the growth when lactate is present as a substrate. Other archaea that thrive in hydrothermal deep-sea sediments such as Bathyarchaeota, Lokiarchaeota, Verstraetearchaeota, Korarchaeota, Helarchaeota and Nezharchaeota also appear to have the genetic potential for methoxytrophic growth. As methoxylated aromatic compounds are quite abundant on earth, especially in the subsurface, we hypothesize that methoxylated aromatic compounds serve as a growth substrate, either on their own or as co-substrate, for more microorganisms than previously assumed and that methoxytrophic growth might play an underestimated role in the global carbon cycle.

Experimental procedures

Cultivation of *Archaeoglobus fulgidus*

Archaeoglobus fulgidus VC-16 (DSM 4304) was cultivated in anoxic, carbonate buffered medium (50 ml medium in 120 ml glass bottles) under an atmosphere of N₂:CO₂ 80:20 (1 atm), at pH 6.8, similar as described by Hocking *et al.* (2014). The composition of the media was as follows: 0.32 g/l KCl, 4.0 g/l MgCl₂ × 6 H₂O, 0.25 g/l NH₄Cl, 0.14 g/l CaCl₂ × 2 H₂O, 0.11 g/l K₂HPO₄, 0.2 g/l KH₂PO₄, 18.0 g/l NaCl, 0.3 g/l yeast extract, 2.5 g/l NaHCO₃, a 100 × trace element solution (1.5 g/l nitrilotriacetic acid, 3 g/l MgSO₄ × 7 H₂O, 0.45 g/l MnSO₄ × 2 H₂O, 1 g/l NaCl, 0.1 g/l FeSO₄ × 7 H₂O, 0.18 g/l CoSO₄ × 6 H₂O, 0.1 g/l CaCl₂ × 2 H₂O, 0.18 g/l ZnSO₄ × 7 H₂O, 0.01 g/l CuSO₄ × 5 H₂O, 0.02 g/l KAl(SO₄)₂

× 12 H₂O, 0.01 g/l H₃BO₃, 0.01 g/l Na₂WO₄ × 2 H₂O, 0.01 g/l Na₂MoO₄ × 2 H₂O, 0.025 g/l NiCl₂ × 6 H₂O, 0.01 g/l Na₂SeO₃) and 0.5 ml/l 0.2% resazurin. Before inoculating, sterile anoxic solutions of cysteine (0.5 mM), Na₂S (0.5 mM), MgSO₄ (16 mM), L-lactate (35 mM) or 2-methoxyphenol (2-MP; 7.5 to 30 mM) were added to the autoclaved medium. Cultivation was performed at 80°C. Next to 2-methoxyphenol also 7.5 mM 2-methoxybenzoate, 3,4,5-trimethoxybenzoate, 2,6-dimethoxyphenol, 3,5-dimethoxy-4-hydroxycinnamic acid, 4-methoxyphenylacetic acid, methoxyhydroquinone, methyl 2-methoxybenzoate and 15 mM methanol were tested as growth substrate. Growth could only be observed with certainty for 2-methoxyphenol, 2,6-dimethoxyphenol, methoxyhydroquinone and 2-methoxybenzoate (Supporting Information Fig. S2). Furthermore, it was tested if *A. fulgidus* can grow without CO₂ with lactate or 2-MP as substrate. Medium without CO₂ was prepared as described above but leaving out NaHCO₃, adding 4.6 g/l piperazine-N,N'-bis(2-ethanesulfonic acid) (PIPES), adjusting the pH to 6.9 and gassing with N₂ instead of N₂-CO₂.

Following growth and substrate consumption of *A. fulgidus*

Growth was followed by measuring the optical density at 600 nm (OD₆₀₀) with a Cary 60 UV-Vis spectrophotometer (Agilent Technologies, USA) at distinct time points. To prevent interference of the absorbance of resazurin, which is present in the medium, sodium dithionite was added to the cuvettes before measuring OD₆₀₀. For all growth conditions, triplicates were used and those triplicates were also used for analysis of substrate consumption/product formation which is described in the following section.

Determination of CO₂ and H₂. The CO₂ and H₂ concentration in the headspace was measured by gas chromatography with a gas chromatograph (Hewlett Packard 5890a, Agilent Technologies, Santa Clara, CA, USA) equipped with a Porapak Q 100/120 mesh and a thermal conductivity detector (TCD) using N₂ as carrier gas. Each measurement was performed by injection of 50 µl headspace gas with a gas-tight syringe. CO₂ concentrations were corrected for the volume removed from the bottle due to OD₆₀₀ measurements. No H₂ production or consumption could be observed.

Determination of methane. To analyse if the cultures produce methane, 50 µl headspace volume were injected with a gas-tight glass syringe (Hamilton, Reno, NE) into an Agilent 6890 series gas chromatograph coupled to a Agilent 5975C mass spectrometer with triple-Axis

detector (GC–MS) (Agilent, Santa Clara, CA) equipped with a Porapak Q column heated at 80°C. No methane production could be observed.

Determination of 2-methoxyphenol and 2-hydroxyphenol. To measure concentrations of 2-methoxyphenol and 2-hydroxyphenol by HPLC an Agilent 1100 HPLC system equipped with a diode array detector (detecting wavelength 260 nm) and a Merck C-18e column (250 mm × 4.6 mm, 5 µm particle size) was used. The flow rate was 0.75 ml/min and a linear gradient was applied: 75% trifluoroacetic acid (TFA) (0.1% in water), 25% acetonitrile to 50% TFA (0.1% in water), 50% acetonitrile in 15 min. A solution of 2-methoxyphenol and 2-hydroxyphenol in water (0.1 mg/ml) was used as standard. Twenty microlitres of sample was used for injection.

Acetate determination. For the determination of acetate concentrations, a slightly modified method of Kage *et al.* (2004) was used. Two hundred microlitres of pentafluorobenzylbromide (PFBBBr) solution (100 mM in acetone) and 40 µl phosphate buffer (0.5 M, pH 6.8) were added to 40 µl sample, mixed and incubated for 1 h at 60°C in an eppendorf tube with safety cap. After cooling down to room temperature, 400 µl hexane (containing 50 µg/ml methylstearate as internal standard) was added and vortexed for 1 min. Thereafter, the sample was centrifuged at 15 000 × *g* for 1 min. From the hexane layer (top), 100 µl was transferred to a GC vial. One microlitre of the sample was used for analysis by GCMS. To determine precise acetate concentrations, a calibration curve was made. A stock solution of 100 mM sodium acetate in water was prepared and diluted in a range between 1 and 40 mM acetate. Of each of these dilutions, 40 µl was used for preparation of a calibration curve. Samples were derivatized as described above for the samples. For analysis of PFBBBr derivatives, an Agilent 7890A gas chromatograph equipped with an autosampler (7693A) and with a JMS-T100GCv JEOL (JEOL) mass spectrometer was used. The gas chromatograph contains a HP-5MS column 30 m × 0.25 mm × 0.25 µm. The following conditions were applied for GC-TOF-MS acetate analysis: The oven temperature was set to 50°C for 2 min, followed by a temperature gradient of 20°C/min to 300°C for 1 min. The split ratio was 1:10 and the detector voltage 2000 V. Peaks were detected by total ion current (TIC) and a selected trace with mass range *m/z* 239.9–240.1 used for detection and quantification of the acetate-PFB derivative. Data were evaluated with Xcalibur (version 2.1, Thermo Scientific) after conversion/export to netCDF by MassCenter JEOL.

Sulfide determination. Ten microlitres of samples were used immediately for sulfide determination with the

methylene blue method by using a sulfide reagent set (HACH, USA; method 8131) according to the manufacturer's instructions. Samples were diluted 100-fold. For calculation of the sulfide concentration the Henry's law constant of 0.001 (mol s² m⁻² kg⁻¹) was used (Sander, 2015). A factor of 2.9 was calculated with the help of this constant and by adjusting for the 80°C incubation temperature to calculate the sulfide concentration in the headspace with help of the following equation $KRT = c(\text{liquid})/c(\text{gasphase})$, where *K* is Henry's law constant, *R* the gas constant and *T* the temperature.

Sulfate determination. Twenty microlitres of samples were used to measure sulfate concentrations with a Sulfate Assay kit (MAK132, Sigma-Aldrich) according to the manufacturer's instructions. Samples were diluted 10-fold.

Formate determination. Five microlitres of samples were used for measuring formate with a Formate Assay kit (MAK059, Sigma-Aldrich) according to the manufacturer's instructions. Samples were diluted 10-fold.

Lactate determination. Lactate was measured after the method described by Borshchevskaya *et al.* (2016). Twenty-five microlitres of sample was mixed with 1 ml 0.2% iron (III) chloride hexahydrate. Using 10 g/l acetate and formate instead of sample leads to Abs₃₉₀ nm value similar to those of the medium background, showing that those compounds do not interfere with the assay. With help of this assay, it was observed that about 23 mM (1.2 mmol per bottle) lactate out of 42 mM (2.1 mmol per bottle) lactate were consumed during the growth of *A. fulgidus*.

Resting cell experiment

A. fulgidus cells grown in 50 ml medium (see above) with 12 mM 2-MP or 35 mM lactate as substrate were harvested anaerobically in the exponential phase and washed with stabilization buffer (2 mM KH₂PO₄/K₂HPO₄, 2 mM MgSO₄, 400 mM NaCl, 200 mM sucrose, pH 6.8, gassed with N₂). The cell pellets were resuspended in 40 ml stabilization buffer (see above) and transferred into 120 ml anaerobic glass bottles. The cultures were incubated for 30 min at 80°C. Afterwards, 6 mM 2-MP or 17 mM lactate and 8 mM MgSO₄ were added and the cultures were incubated for 5 h at 80°C. The CO₂ gas produced by the cultures was analysed every hour by injecting 50 µl headspace volume with a gas-tight glass syringe (Hamilton, Reno, NE) into an Agilent 6890 series gas chromatograph coupled to a mass spectrometer (GC–MS) (Agilent, Santa Clara, CA) equipped with a Porapak Q column heated at 80°C. For calculating the

CO₂ in the culture headspace, a calibration curve was generated by injecting different volumes of calibration gas (Linde Gas Benelux) that contained 1% CO₂ and 1% CH₄ into the GC–MS. The CO₂ values (in %) were corrected for the CO₂ in the medium in form of HCO₃[–] by measuring the headspace CO₂ in 40 ml buffer before and after acidification with HCl. The experiment was performed in triplicate. Values for CO₂ production were adjusted to the protein content of each sample. For the protein determination, 500 µl of cells were sampled at *t*₀ and boiled for 15 min at 110°C. Afterwards, 2 ml –20°C cold acetone was added and the samples incubated at –20°C for 1 h. The samples were centrifuged at 20 000 × *g* for 15 min, the supernatant removed and the pellets dried for 30 min at room temperature. After resuspending the pellets in 50 µl H₂O, the protein content was measured by the Bradford Protein Assay (5000006, Bio-Rad) according to the manufacturer's instructions.

Metabolite analysis of A. fulgidus cells grown under different conditions

A. fulgidus was grown in triplicates in 50 ml medium (see above) with either 12 mM 2-MP (Mp), 35 mM lactate (Lac) or 12 mM 2-MP plus 35 mM lactate (M + L). As a control, a culture without substrate was used (no change in OD₆₀₀). Cells were harvested aerobically in the exponential phase (OD₆₀₀ MP: 0.06, Lac: 0.13, M + L: 0.15) at 20 000 × *g* and 4°C for 15 min. Pellets were washed with 1 ml cold PBS and centrifuged for 1 min at 12 000 × *g*. The remaining pellet was lysed using 500 µl of H₂O: methanol:acetonitrile(40:40:20, V:V:V). After centrifugation for 1 min at 12 000 × *g*, the supernatant was transferred into a fresh tube and stored at –20°C until metabolite analysis. Aqueous normal phase metabolomics was performed on 2 µl sample using a 1290 Infinity II LC system coupled to a 6546 Q-ToF MS (Agilent Technologies) as previously described (Jansen *et al.*, 2020). In brief, samples were injected onto a Diamond Hydride Type C column (Cogent) and separated using a gradient of water and acetonitrile with 0.2% formic acid. Detection was performed in the negative ionization mode from *m/z* 50–1200. For the detection of glutamate, samples were diluted 20-fold in acetonitrile: methanol:water (40:40:20, V:V:V) to overcome sodium-related interferences. Metabolites were identified based on MS fragmentation and quantified using Qualitative Analysis 10.0 (Agilent Technologies). Metabolite signals were normalized for OD₆₀₀.

RNA isolation from A. fulgidus cells

Cultures for RNA extractions/transcriptomics were grown in 250 ml medium with either 10 mM 2-MP or 35 mM

lactate. Cells were harvested anaerobically in the exponential phase at 10 000 × *g*, 20 min and 4°C. The pellet was frozen in liquid nitrogen and stored at –80°C until RNA isolation. RNA isolation was performed with the RiboPure-Bacteria Kit (Thermo Fischer Scientific) according to the manufacturer's instructions. Quantity and quality of RNA from lactate and 2-MP grown cells (in triplicates) were checked with an Agilent 2100 Bioanalyzer and the RNA Integrity Number was between 7.2 and 8.2.

Transcriptome sequencing and analyses

For library preparation, the TruSeq[®] Stranded mRNA Library Prep protocol (Illumina, San Diego, CA, USA) was used according to the manufacturer's instructions. Total RNA was used for library preparation. The library concentration measured with a Qubit fluorometer and the average fragment size obtained with the Agilent 2100 Bioanalyzer were used to calculate the correct dilution factor required for normalization of the library. After dilution to 4 nM and denaturation using the Denature and Dilute Libraries Guide (Illumina, San Diego, CA), the library was sequenced using an Illumina MiSeq machine (San Diego, CA) to generate 150 bp single-end reads.

To analyse transcriptomic data, raw reads from the MiSeq platform were initially trimmed based on a quality limit of 0.02 and minimal length of 50 bp using the CLC Genomics Workbench 12 (Qiagen, Aarhus, Denmark). Next, RNA reads were mapped to the draft genome of *A. fulgidus* DSM 4304 AE000782.1 (insertion cost, 3; deletion cost, 3; length fraction, 0.8; similarity fraction, 0.95). Further analysis was conducted with RStudio using R package 'Deseq2' (Love *et al.*, 2014). The gene expression values were expressed as RPKM (Reads per kilo base of exon model per million mapped reads) and log₂fold change values. For the generation of the heat map, RPKM values were imported into RStudio v. 1.2.5033 (using R v. 4.0.3), and the packages RColorBrewer v. 1.1.2, gplots v. 3.1.1 and vegan v. 2.5.6 were used, with the function 'heatmap.2'.

Protein sequence analyses

We identified relevant archaeal sequences via BlastP using *A. fulgidus* amino acid sequences of MtoABCD, blasting them against the non-redundant blast database and we selected sequences with at least 35% amino acid identity coming from one same genome (*Candidatus* Bathyarchaeota archaeon SpSt-709: DTEF01, *Candidatus* Verstraetearchaeota archaeon SJ3.Bin21: JAAOZJ01, *Candidatus* Nezhaarchaeota archaeon WYZ-LMO8: QNVF01, *Candidatus* Lokiarchaeota archaeon Hel_238_bin90: JABXKC01, *Candidatus* Helarchaeota

archaeon CR_Bin_143: JABXJV01, *Candidatus* Korarchaeota archaeon B41_G2: QMVX01). Improved protein annotation was obtained via NCBI blast analysis (<https://blast.ncbi.nlm.nih.gov/Blast.cgi?PAGE=Proteins>). The phylogenetic tree was generated via multiple alignment of amino acid sequences retrieved from NCBI with MUSCLE (Edgar, 2004) v. 3.8.31 (sequence accession numbers are provided in the tree). Alignment columns were stripped with trimAl (Capella-Gutiérrez *et al.*, 2009) v. 1.4.rev22 using the -gappout option, and the tree was built with FastTree (Price *et al.*, 2010) v.2.1.10 using the Jones-Taylor-Thorton maximum likelihood model. The tree was visualized with iTOL (Letunic and Bork, 2019) v.4 and edited on Adobe Illustrator CC 2018 (San Jose, California, USA).

Data availability

The transcriptomics data have been deposited at the Sequence Read Archive (SRA) from NCBI with BioProject accession number PRJNA695423 under the following link: <https://www.ncbi.nlm.nih.gov/sra/PRJNA695423>.

Acknowledgements

CUW, JMK and MSMJ were supported by the Nederlandse Organisatie voor Wetenschappelijk Onderzoek through the Soehngen Institute of Anaerobic Microbiology (SIAM) Gravitation Grant 024.002.002. MSMJ was further supported by the Netherlands Earth System Science Center Gravitation Grant 024.002.001 and the European Research Council Advanced Grant Ecology of Anaerobic Methane Oxidizing Microbes 339880. JMK was supported by the Deutsche Forschungsgesellschaft (DFG) Grant KU 3768/1-1. We thank Theo van Alen and Geert Cremers for technical assistance. We further thank Ines A.C. Pereira and Sofia Venceslau for sending us *A. fulgidus* strain VC-16, Garrett Smith for helping with the transcriptomic analysis and William Hocking for providing the raw data of the Hocking *et al.* (2014) and (2015) studies.

References

- Bache, R., and Pfennig, N. (1981) Selective isolation of *Acetobacterium woodii* on methoxylated aromatic acids and determination of growth yields. *Arch Microbiol* **130**: 255–261.
- Beeder, J., Nilsen, R.K., Rosnes, J.A.N.T., Torsvik, T., and Lien, T. (1994) *Archaeoglobus fulgidus* isolated from hot North Sea oil field waters. *Appl Environ Microbiol* **60**: 1227–1231.
- Berg, I.A., Kockelkorn, D., Buckel, W., and Fuchs, G. (2007) Autotrophic carbon dioxide assimilation pathway in archaea. *Science* **318**: 1782–1786.

- Borshchevskaya, L.N., Gordeeva, T.L., Kalina, A.N., and Sineokii, S.P. (2016) Spectrophotometric determination of lactic acid. *J Anal Chem* **71**: 755–758.
- Breznak, J.A., Switzer, J.M., and Seitz, H.-J. (1988) *Sporomusa termitida* sp. nov., an H₂/CO₂-utilizing acetogen isolated from termites. *Arch Microbiol* **150**: 282–288.
- Burdige, D.J. (2005) Burial of terrestrial organic matter in marine sediments: a re-assessment. *Global Biogeochem Cycles* **19**: 1–7.
- Capella-Gutiérrez, S., Silla-Martínez, J.M., and Gabaldón, T. (2009) trimAl: a tool for automated alignment trimming in large-scale phylogenetic analyses. *Bioinformatics* **25**: 1972–1973.
- Colberg, P.J. (1988) Anaerobic microbial degradation of cellulose, lignin, oligolignols, and monoaromatic lignin derivatives. In *Biology of Anaerobic Microorganisms*, Zehnder, A.J.B. (ed). New York: John Wiley & Sons, pp. 333–372.
- Edgar, R.C. (2004) MUSCLE: multiple sequence alignment with high accuracy and high throughput. *Nucleic Acids Res* **32**: 1792–1797.
- Ertel, J.R., and Hedges, J.I. (1984) The lignin component of humic substances: distribution among soil and sedimentary humic, fulvic, and base-insoluble fractions. *Geochim Cosmochim Acta* **48**: 2065–2074.
- Estelmann, S., Ramos-vera, W.H., Gad, N., Huber, H., Berg, I.A., and Fuchs, G. (2011) Carbon dioxide oxidation in '*Archaeoglobus lithotrophicus*': are there multiple autotrophic pathways? *FEMS Microbiol Lett* **319**: 65–72.
- Grech-Mora, I., Fardeau, M.-L., Patel, B.K.C., Ollivier, B., Rimbault, A., Prensier, G., *et al.* (1996) Isolation and characterization of *Sporobacter termitidis* gen. nov., sp. nov., from the digestive tract of the wood-feeding termite *Nasutitermes lujae*. *Int J Syst Bacteriol* **46**: 512–518.
- Habicht, K.S., Salling, L., Thamdrup, B., and Canfield, D.E. (2005) Effect of low sulfate concentrations on lactate oxidation and isotope fractionation during sulfate reduction by *Archaeoglobus fulgidus* strain Z. *Appl Environ Microbiol* **71**: 3770–3777.
- He, Y., Li, M., Perumal, V., Feng, X., Fang, J., Xie, J., *et al.* (2016) Genomic and enzymatic evidence for acetogenesis among multiple lineages of the archaeal phylum Bathyarchaeota widespread in marine sediments. *Nat Microbiol* **1**: 1–9.
- Healy, J.B., and Young, L.Y. (1979) Anaerobic biodegradation of eleven aromatic compounds to methane. *Appl Environ Microbiol* **38**: 84–89.
- Hedges, J.I., Ertel, J.R., and Leopold, E.B. (1982) Lignin geochemistry of a late quaternary sediment core from Lake Washington. *Geochim Cosmochim Acta* **46**: 1869–1877.
- Henstra, A.M., Dijkema, C., and Stams, A.J.M. (2007) *Archaeoglobus fulgidus* couples CO oxidation to sulfate reduction and acetogenesis with transient formate accumulation. *Environ Microbiol* **9**: 1836–1841.
- Hocking, W.P., Roalkvam, I., Magnussen, C., Stokke, R., and Steen, I.H. (2015) Assessment of the carbon monoxide metabolism of the hyperthermophilic sulfate-reducing archaeon *Archaeoglobus fulgidus* VC-16 by comparative transcriptome analyses. *Archaea* **2015**: 1–12.

- Hocking, W.P., Stokke, R., Roalkvam, I., and Steen, I.H. (2014) Identification of key components in the energy metabolism of the hyperthermophilic sulfate-reducing archaeon *Archaeoglobus fulgidus* by transcriptome analyses. *Front Microbiol* **5**: 1–20.
- Hua, Z.-S., Wang, Y.-L., Evans, P.N., Qu, Y.-N., Goh, K.M., Rao, Y., et al. (2019) Insights into the ecological roles and evolution of methyl-coenzyme M reductase-containing hot spring Archaea. *Nat Commun* **10**: 1–11.
- Jansen, R.S., Mandyoli, L., Hughes, R., Wakabayashi, S., Pinkham, J.T., Selbach, B., et al. (2020) Aspartate aminotransferase Rv3722c governs aspartate-dependent nitrogen metabolism in *Mycobacterium tuberculosis*. *Nat Commun* **11**: 1960.
- Kage, S., Kudo, K., Ikeda, H., and Ikeda, N. (2004) Simultaneous determination of formate and acetate in whole blood and urine from humans using gas chromatography-mass spectrometry. *J Chromatogr B* **805**: 113–117.
- Kaufmann, F., Wohlfarth, G., and Diekert, G. (1997) Isolation of O-demethylase, an ether-cleaving enzyme system of the homoacetogenic strain MC. *Arch Microbiol* **168**: 136–142.
- Khelifi, N., Grossi, V., Hamdi, M., Dolla, A., Tholozan, J.-L., Ollivier, B., and Hirschler-Réa, A. (2010) Anaerobic oxidation of fatty acids and alkenes by the hyperthermophilic sulfate-reducing archaeon *Archaeoglobus fulgidus*. *Appl Environ Microbiol* **76**: 3057–3060.
- Klenk, H.P., Clayton, R.A., Tomb, J.F., White, O., Nelson, K. E., Ketchum, K.A., et al. (1997) The complete genome sequence of the hyperthermophilic, sulphate-reducing archaeon *Archaeoglobus fulgidus*. *Nature* **390**: 364–370.
- Konn, C., Charlou, J.L., Donval, J.P., Holm, N.G., Dehairs, F., and Bouillon, S. (2009) Hydrocarbons and oxidized organic compounds in hydrothermal fluids from rainbow and lost city ultramafic-hosted vents. *Chem Geol* **258**: 299–314.
- Kurth, J.M., Nobu, M.K., Tamaki, H., de Jonge, N., Berger, S., Jetten, M.S.M., et al. (submitted) Methanogenic archaea use a bacteria-like methyltransferase system to demethoxylate aromatic compounds. *ISME J*.
- Lee, H., Feng, X., Mastalerz, M., and Feakins, S.J. (2019) Characterizing lignin: combining lignin phenol, methoxy quantification, and dual stable carbon and hydrogen isotopic techniques. *Org Geochem* **136**: 103894.
- Letunic, I., and Bork, P. (2019) Interactive tree of life (iTOL) v4: recent updates and new developments. *Nucleic Acids Res* **47**: 256–259.
- Libes, S.M. (2009) The origin of petroleum in the marine environment. In *Introduction to Marine Biogeochemistry*. Amsterdam: Elsevier Science, pp. 1–33.
- Liebensteiner, M.G., Pinkse, M.W.H., Schaap, P.J., Stams, A.J.M., and Lomans, B.P. (2013) Archaeal (per)chlorate reduction at high temperature: an interplay of biotic and abiotic reactions. *Science* **340**: 85–87.
- Liebensteiner, M.G., Stams, A.J.M., and Lomans, B.P. (2014) (Per)chlorate reduction at high temperature: physiological study of *Archaeoglobus fulgidus* and potential implications for novel souring mitigation strategies. *Int Biodeterior Biodegrad* **96**: 216–222.
- Lomans, B.P., Leijdekkers, P., Wesselink, J.-J., Bakkes, P., Pol, A., van der Drift, C., and Op den Camp, H.J.M. (2001) Obligate sulfide-dependent degradation of methoxylated aromatic compounds and formation of methanethiol and dimethyl sulfide by a freshwater sediment isolate, *Parasporobacterium paucivorans* gen. Nov., sp. nov. *Appl Environ Microbiol* **67**: 4017–4023.
- Love, M.I., Huber, W., and Anders, S. (2014) Moderated estimation of fold change and dispersion for RNA-seq data with DESeq2. *Genome Biol* **15**: 1–21.
- Maksymiuk, C., Balakrishnan, A., Maksymiuk, C., Balakrishnan, A., Bryk, R., Rhee, K.Y., and Nathan, C.F. (2015) E1 of α -ketoglutarate dehydrogenase defends *Mycobacterium tuberculosis* against glutamate anaplerosis and nitroxidative stress. *Proc Natl Acad Sci U S A* **112**: E5834–E5843.
- Mayumi, D., Mochimaru, H., Tamaki, H., Yamamoto, K., Yoshioka, H., Suzuki, Y., et al. (2016) Methane production from coal by a single methanogen. *Science* **354**: 222–225.
- Mechichi, T., Labat, M., Garcia, J.-L., Thomas, P., and Pate, B.K.C. (1999) *Sporobacterium olearium* gen. Nov., sp. nov., a new methanethiol-producing bacterium that degrades aromatic compounds, isolated from an olive mill wastewater treatment digester. *Int J Syst Bacteriol* **49**: 1741–1748.
- Meslé, M., Dromart, G., and Oger, P. (2013) Microbial methanogenesis in subsurface oil and coal. *Res Microbiol* **164**: 959–972.
- Möller-Zinkhan, D., Börner, G., and Thauer, R.K. (1989) Function of methanofuran, tetrahydromethanopterin, and coenzyme F420 in *Archaeoglobus fulgidus*. *Arch Microbiol* **152**: 362–368.
- Möller-Zinkhan, D., and Thauer, R.K. (1990) Anaerobic lactate oxidation to 3 CO₂ by *Archaeoglobus fulgidus* via the carbon monoxide dehydrogenase pathway: demonstration of the acetyl-CoA carbon-carbon cleavage reaction in cell extracts. *Arch Microbiol* **153**: 215–218.
- Odom, J.M., and Peck, H.D. (1981) Hydrogen cycling as a general mechanism for energy coupling in the sulfate-reducing bacteria, *Desulfovibrio* sp. *FEMS Microbiol Lett* **12**: 47–50.
- Parthasarathy, A., Kahnt, J., Chowdhury, N.P., and Buckel, W. (2013) Phenylalanine catabolism in *Archaeoglobus fulgidus* VC-16. *Arch Microbiol* **195**: 781–797.
- Pierce, E., Xie, G., Barabote, R.D., Saunders, E., Han, C.S., Detter, J.C., et al. (2008) The complete genome sequence of *Moorella thermoacetica* (f. *Clostridium thermoaceticum*). *Environ Microbiol* **10**: 2550–2573.
- Price, M.N., Dehal, P.S., and Arkin, A.P. (2010) FastTree 2—approximately maximum-likelihood trees for large alignments. *PLoS One* **5**: 1–10.
- Salmon, V., Derenne, S., Largeau, C., Beaudoin, B., Bardoux, G., and Mariotti, A. (1997) Kerogen chemical structure and source organisms in a Cenomanian organic-rich black shale (Central Italy)—indications for an important role of the “sorpitive protection” pathway. *Org Geochem* **27**: 423–438.
- Sander, R. (2015) Compilation of Henry’s law constants (version 4.0) for water as solvent. *Atmos Chem Phys* **15**: 4399–4981.

- Seitz, K.W., Dombrowski, N., Eme, L., Spang, A., Lombard, J., Sieber, J.R., *et al.* (2019) Asgard archaea capable of anaerobic hydrocarbon cycling. *Nat Commun* **10**: 1822.
- Stetter, K.O. (1988) *Archaeoglobus fulgidus* gen. Nov., sp. nov.: a new taxon of extremely thermophilic Archaeobacteria. *Syst Appl Microbiol* **10**: 172–173.
- Stetter, K.O., and Huber, R. (1998) The role of hyperthermophilic prokaryotes in oil fields. In *Microbial Biosystems: New Frontiers*, Bell, C.R., Brylinsky, M., and Johnston-Green, P. (eds). Halifax: Atlantic Canada Society for Microbial Ecology, pp. 369–375.
- Stetter, K.O., Lauerer, G., Thomm, M., and Neuner, A. (1987) Isolation of extremely thermophilic sulfate reducers: evidence for a novel branch of archaeobacteria. *Science* **236**: 822–825.
- Toso, D.B., Javed, M.M., Czornyj, E., Gunsalus, R.P., and Zhou, Z.H. (2016) Discovery and characterization of iron sulfide and polyphosphate bodies coexisting in *Archaeoglobus fulgidus* cells. *Archaea* **2016**: 1–11.
- Wang, W., Li, Z., Zeng, L., Dong, C., and Shao, Z. (2020) The oxidation of hydrocarbons by diverse heterotrophic and mixotrophic bacteria that inhabit deep-sea hydrothermal ecosystems. *ISME J* **14**: 1994–2006.
- Wang, Y., Wegener, G., Hou, J., Wang, F., and Xiao, X. (2019) Expanding anaerobic alkane metabolism in the domain of archaea. *Nat Microbiol* **4**: 595–602.
- Welte, C.U. (2016) A microbial route from coal to gas. *Science* **354**: 184–184.
- Wiechmann, A., Ciurus, S., Oswald, F., Seiler, V.N., and Müller, V. (2020) It does not always take two to tango: “Syntrophy” via hydrogen cycling in one bacterial cell. *ISME J* **14**: 1561–1570.
- Wu, Z., Daniel, S.L., and Drake, H.L. (1988) Characterization of a CO-dependent O-demethylating enzyme system from the acetogen *Clostridium thermoaceticum*. *J Bacteriol* **170**: 5747–5750.
- Yin, X., Cai, M., Liu, Y., Zhou, G., Aromokeye, D.A., Kulkarni, A.C., *et al.* (2020) Subgroup level differences of physiological activities in marine Lokiarchaeota. *ISME J* **15**: 848–861.
- Yu, T., Wu, W., Liang, W., Alexander, M., and Hinrichs, K.-U. (2018) Growth of sedimentary Bathyarchaeota on lignin as an energy source. *Proc Natl Acad Sci U S A* **115**: 6022–6027.
- Zeikus, J.G. (1981) Lignin metabolism and the carbon cycle. In *Advances in Microbial Ecology*, Alexander, M. (ed). Boston (MA): Springer, pp. 211–243.

Supporting Information

Additional Supporting Information may be found in the online version of this article at the publisher's web-site:

Appendix S1: Supporting information.